The Effectiveness of Path-Segmentation for Modeling Lasso Times in Width-Varying Paths

SHOTA YAMANAKA, Yahoo Japan Corporation, Japan
HIROKI USUBA, Yahoo Japan Corporation, Japan
WOLFGANG STUERZLINGER, Simon Fraser University, Canada
HOMEI MIYASHITA, Meiji University, Japan

Models of lassoing time to select multiple square icons exist, but realistic lasso tasks also typically involve encircling non-rectangular objects. Thus, it is unclear if we can apply existing models to such conditions where, e.g., the width of the path that users want to steer through changes dynamically or step-wise. In this work, we conducted two experiments where the objects were non-rectangular, with path widths that narrowed or widened, smoothly or step-wise. The results showed that the baseline models for pen-steering movements (the steering and crossing law models) fitted the timing data well, but also that segmenting width-changing areas led to significant improvements. Our work enables the modeling of novel UIs requiring continuous strokes, e.g., for grouping icons.

CCS Concepts: • **Human-centered computing → HCI theory, concepts and models**; **Empirical studies in HCI**.

Additional Key Words and Phrases: Graphical user interfaces, human motor performance modeling, lassoing, steering

ACM Reference Format:
Shota Yamanaka, Hiroki Usuba, Wolfgang Stuerzlinger, and Homei Miyashita. 2022. The Effectiveness of Path-Segmentation for Modeling Lasso Times in Width-Varying Paths. *Proc. ACM Hum.-Comput. Interact.* 6, ISS, Article 584 (December 2022), 20 pages. https://doi.org/10.1145/3567737

1 INTRODUCTION

1.1 Background

Graphical user interfaces (GUIs) typically support several methods to select multiple objects. Most systems support drawing a rectangle area by crossing the intended objects group diagonally or clicking on several objects while keeping a modifier key pressed, e.g., `ctrl`. Some illustration software, presentation tools, and photo managers also provide *lasso selection*, which involves performing a continuous encircling stroke around the intended objects. Researchers also have examined lasso variants to improve user performance. Examples include automatically connecting the start and end points [23] and considering the likelihood of objects belonging to the same group [12].

When researchers develop a novel technique for GUI operations, it is beneficial to do this based on a good theoretical understanding of the new method, aided by human performance models

Authors' addresses: Shota Yamanaka, Yahoo Japan Corporation, Tokyo, Japan, syamanak@yahoo-corp.jp; Hiroki Usuba, Yahoo Japan Corporation, Tokyo, Japan, c-hiusuba@yahoo-corp.jp; Wolfgang Stuerzlinger, Simon Fraser University, Vancouver, Canada, w.s@sfu.ca; Homei Miyashita, Meiji University, Tokyo, Japan, homei@homei.com.

Permission to make digital or hard copies of all or part of this work for personal or classroom use is granted without fee provided that copies are not made or distributed for profit or commercial advantage and that copies bear this notice and the full citation on the first page. Copyrights for components of this work owned by others than the author(s) must be honored. Abstracting with credit is permitted. To copy otherwise, or republish, to post on servers or to redistribute to lists, requires prior specific permission and/or a fee. Request permissions from permissions@acm.org.
© 2022 Copyright held by the owner/author(s). Publication rights licensed to ACM.
2573-0142/2022/12-ART584 $15.00
https://doi.org/10.1145/3567737

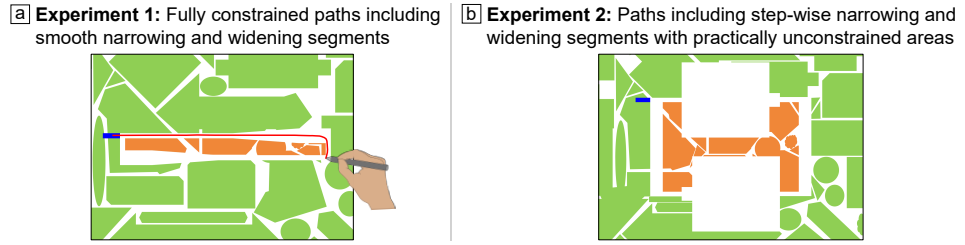

Fig. 1. The two lassoing tasks tested in this study. Starting at the blue area, the participants had to circle all orange objects by passing through the white empty regions. As we counted touching orange or green objects as an error, they had to move the stylus carefully in narrow path areas, while they could accelerate in wider area to shorten the movement time.

such as Fitts' law [14]. However, for lassoing tasks, established models predict limited conditions, specifically only square icons in a grid and only a constant path width throughout the task [10, 45]. This type of arrangements is a special case for lassoing, e.g., in group selection in file or photo managers. In illustration software or note-taking tools, objects are not limited to squares, and object positions are often not aligned to a grid. Thus, it is unclear whether lassoing times can be accurately modeled by existing models.

1.2 Hypothesis and Contribution

Some previous studies on lasso-time models [45, 47] segmented a given path to be steered into a number of portions so that existing pen-based movement time (MT) prediction models could be applied, including Fitts' law [14], the steering law [1], and the crossing law models [4]. Although these studies showed that this approach could predict the MTs more accurately than no-segmentation methods, i.e., interpreting a lasso task as a single path-steering motion, these studies used only equally sized icons that created constant-width paths. Thus the applicability of this approach to more realistic situations such as lassoing tasks where path varies in width is questionable. If the approach of path segmentation [45, 47] is effective for more complicated path shapes, we hypothesize as follows.

- **Hypothesis**: With width-varying lasso paths, the MTs can be predicted more accurately by segmenting the path compared to using the global steering law model.

To test this hypothesis, we conducted two experiments where the lasso path varies in width, either smoothly or abruptly, while still being experimentally controlled (Figure 1). By integrating the findings across the results of the two experiments, we found that, even for complex lasso paths, the MTs can be predicted by carefully segmenting the lasso path into smaller elements, each of which can be modeled with existing human performance models. Thus our contribution of this study is to address limitation of previous work: the path-segmentation approach can generalize lasso-time predictions to tasks that involve non-rectangular objects in note-taking tools or illustration software. As previous work had only demonstrated that modeling MTs by path-segmentation is effective only for equally sized square objects arranged in a grid, i.e., severely constrained task conditions, it is (at best) unclear if that approach generalizes to more complex lasso paths.

1.3 Scope of the Present Study

The scope of our work presented here does not include a unified model that can be generalized to all lasso tasks – this is still a major challenge, which involves too many factors that may need to be considered, such as curved paths, the potential effects of object colors or object features at

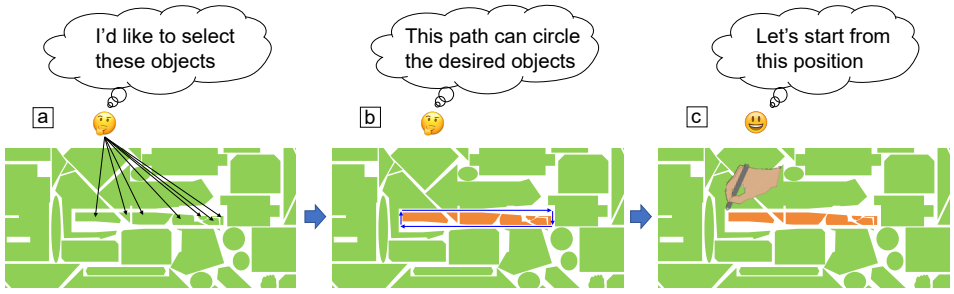

Fig. 2. In realistic scenarios, users have to go through several steps to accomplish a lasso task, such as (a) deciding which objects to select, (b) determining an appropriate path to select them, and (c) pointing to the position to start the lasso operation (i.e., a Fitts' law task). As we aim to model the time required for the main lassoing motions, the time (and cognitive load) required for all the preparatory steps in this figure are out of scope for the work presented here. Thus, the desired objects are highlighted in orange, the direction to be steered is fixed to be clockwise, and the starting position is given.

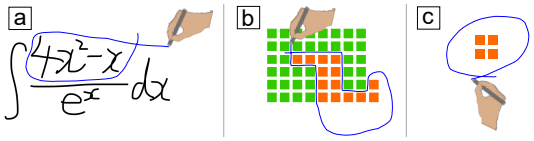

Fig. 3. Example tasks having partially or fully unconstrained areas to be stroked, whose time prediction models have been examined in previous studies. Thus, we do not test such scenarios in this work. (a) *Sloppy selection* technique in which a user wants to select only the numerator in a note-taking tool [21]. (b) Lassoing a group of icons that involves both constrained and unconstrained areas [45]. (c) A lasso operation where users do not have to pay attention to distractors [15, 38].

different scales. To progress towards the goal of a general model for lasso times and building on the state-of-the art [45], we identify how one needs to account for critical factors, such as path shape, to predict lasso times more accurately. As we designed the task conditions for each of the experiments presented here to examine specific, but different task factors, we expect that the best model for each experiment (and thus type of path segment) naturally has a different formulation. As our overarching goal for this work is to investigate the strategy of path segmentation, this is an expected and acceptable outcome.

In realistic tasks, however, several steps are needed to plan and execute a lasso motion. Some users may determine which objects in the forward direction are to be selected while moving the stylus, while other users may decide the desired objects a priori and then execute the lasso operation as a whole. For modeling the first case, various cognitive factors potentially affect user performance, including the potential similarity and proximity of objects (cf. the Gestalt laws), or locations where users have to make decisions on which path to follow. Such factors make prediction hard and thus we consider such tasks to be outside of the scope of our current work. Therefore, we also do not investigate the time taken by the user before beginning a stroke, such as the processes shown in Figure 2. To focus on modeling human motor performance in predetermined lassoing tasks, we designed our experimental tasks so that the objects to be selected and non-target ones are shown in two easily distinguishable colors.

As our focus is on the baseline performance of lasso operations, we did not use supporting lasso techniques, such as auto-closing the stroke. Another type of lasso tool, typically used for segmenting

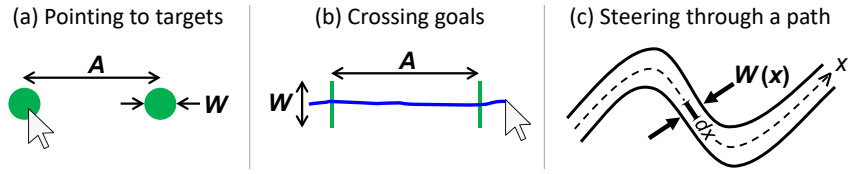

Fig. 4. Illustration of the three elemental operations that form the basis for our models. (a) Pointing to targets and (b) crossing goals are both modeled by Fitts' law. (c) Steering through a constrained path is modeled by the steering law.

an area from a photo, based on edge detection, e.g., in *GrabCut* [29], is also out of scope of our work. Also, models for lasso tasks which include partially or fully unconstrained areas (see Figure 3) have been presented in previous work. Thus, we focus in our first experiment on conditions where the pen-tip movements are constrained throughout the lasso motion. In our experiment 2 we then expand our investigation to include very wide path segments that are effectively unconstrained.

2 RELATED WORK

2.1 Measurement of Task Completion Times for Lassoing Tasks

Basic lassoing performance has been evaluated in the past, often in comparisons with novel techniques [10, 12, 23, 41]. To predict baseline user performance, Bjerre et al. proposed a model linear in the number of lassoed icons [10]. At best, it is unclear if such a simplistic model can handle different icon shapes or free areas, when one considers, e.g., that their model predicts the same time for two tiny icons and a huge and a tiny ones. Yamanaka and Stuerzlinger conducted two experiments with square icons arranged in a grid, where some path segments optionally involved free space [45]. For the fully constrained condition, the lasso task was reasonably modeled by a steering motion, but a segmented model with successive steering motions showed an even better fit. For the partially constrained condition, the crossing model [4] further improved time prediction accuracy for entering an constrained area from an unconstrained one.

2.2 Performance Models for GUI Operations

2.2.1 Pointing and Crossing Models. MacKenzie's formulation [22] of Fitts' law [14] is widely used in HCI to predict the *MT* of pointing tasks:

$$MT = a_p + b_p ID_p, \quad ID_p = \log_2 (A/W + 1) \tag{1}$$

where A is the distance to the target, W is the target size, and a_p and b_p are empirical constants for pointing (see Figure 4a). The logarithmic term is called the *index of difficulty* of pointing (ID_p).

Crossing a goal line is also modeled by Fitts' law [4]. Given a goal length W and a distance A, the time is predicted as: $MT = a_c + b_c ID_c$, where $ID_c = \log_2(A/W + 1)$ and a_c and b_c are crossing regression constants (see Figure 4b). Yamanaka et al. used the crossing model to predict the time to enter a "gate" between obstacles from wider to narrower path segments [46] and between unconstrained and constrained areas [45, 47].

2.2.2 Steering Model. Models for steering through a given path have been proposed several times [1, 13, 28]. Accot and Zhai [1] proposed a global steering law model to pass through a path (or tunnel) T:

$$MT = a_s + b_s ID_s, \quad ID_s = \int_T \frac{dx}{W(x)} \tag{2}$$

where x is the cursor position in the path, $W(x)$ is the path width at x, and a_s and b_s are steering constants (see Figure 4c). The integral term is called the steering *index of difficulty* ID_s. If the width W is constant throughout the path, the model simplifies to $MT = a_s + b_s(A/W)$, where A is the path length. This model holds for various devices [2] and movement angles [35, 36], and thus applies to lassoing tasks with various steering directions [45].

For a narrowing straight path, the MT prediction model can be derived from Equation 2:

$$MT = a_s + b_s ID_s, \quad ID_s = \frac{A}{W_2 - W_1} \ln \frac{W_2}{W_1} \tag{3}$$

where W_1 and W_2 are the widths at the start and end of the path. The same model is also valid for a widening straight path, but with different a_s and b_s constants [42, 43].

Based on the mentioned models, given the results for a specific condition, and within reasonable limits, it is possible to predict the performance for any type of task mentioned in Sections 2.1 and 2.2. This is particularly relevant if researchers want to identify the MTs for a new task condition, e.g., how does the MT change if W increases from 5 mm to 10 mm?. One feature of the performance models we work on is that researchers can then accurately predict the average MT when a group of users encounters a new condition. Hence, the resulting models are reusable without performing additional user studies, which is beneficial for researchers designing novel lasso interaction techniques.

2.3 Object Inclusion Criterion for Lassoing

Often, objects inside of the loop or those crossed by the stroke are selected, as in *Illustrator*. Another common criterion selects only objects inside the lasso loop that are not touched by the stroke, as in *OneNote*. A third criterion uses only object center points [23]. With different criteria, only the path width between icons changes and thus the MTs might differ. This difference results in different model coefficients, but the steering law model holds overall *internally* across these three criteria [37]. Participants normally get familiar with a given criterion after sufficient practice.

Consistent with previous work [1, 45, 47], we match here the visual appearance of the path to the task tolerance requirement, i.e., participants cannot touch any objects, which eliminates the corresponding ambiguity for users. If other criteria such as the center-point rule [23] are used, the path width and length only need to be recalculated to take the corresponding variation into account.

3 EXPERIMENT 1: PATHS INCLUDING SMOOTH NARROWING AND WIDENING SEGMENTS

In this Experiment 1, the lasso path included two width-varying segments: called seg2 and seg6 in Figure 5. The *Shape* of these areas were either *Constant*, *Narrowing*, and *Widening*. As the effect of the number of corners had been already investigated [45], we fixed the overall lasso path to be a rectangle consisting of four straight path segments. Based on previous work for single segments [42, 43], we hypothesize that the *Shape* of the path and the corresponding changes of path width would significantly affect MT and error rate.

3.1 Participants and Apparatus

Twelve participants were recruited from a local university (3 female, 9 male; M = 22.1 and SD = 1.26 years). All were right-handed. Each participant received the equivalent of 46 USD.

We used an Apple MacBook Pro laptop (2.8 GHz i5-4308U; 8 GB; macOS Sierra). The input device and display was a Wacom Cintiq 27QHD DTK-2700/K0 (27”, 597.7×336.2 mm, at 2560 × 1440 pixels, 60 Hz refresh). This system reads and processes input about 100 times per second. The

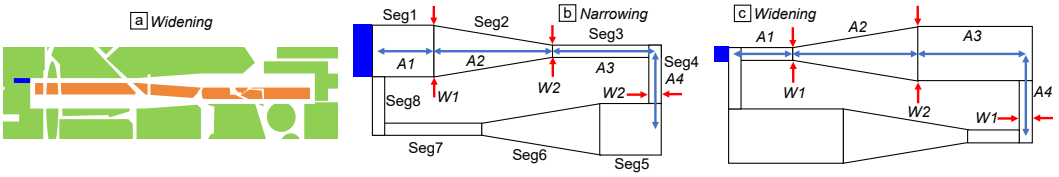

Fig. 5. Path parameter definitions in Experiment 1. With the exception of the width-varying segments (i.e., seg2 and seg6), all other segments had constant width.

tablet was positioned on a table in "stand" mode (20° tilt). The display rejected finger touches. The experimental system was implemented with JavaScript and used in full-screen mode.

3.2 Task

Starting from a blue start area, the task involved making a stroke around all orange objects, see Figure 5a. Participants were asked to perform a quick stroke as long as they did not "touch" any objects, which emphasized accuracy over speed. They were also asked to pass only through the white path. When the pen tip crossed the stroke itself and all orange objects were included in the loop, we played a bell sound to signal success. If participants touched objects or lifted the pen, we played a beep sound and they had to immediately redo the trial with the same path configuration.

To simulate a collection of non-rectangular objects, we created a background image by randomly arranging PowerPoint shapes. Then, we overlaid a white lasso path consisting of eight segments as shown in Figure 5b and c. The lengths of offsets between objects were always shorter than $5W$; thus participants had to use a continuous path-steering motion [30, 47]. Movement direction was always clockwise.

To compensate for any effect due to hand occlusion on the path, we used the same path shapes for both halves in a task. Thus, within the first four path segments (seg1 to seg4 in Figure 5), the width-change always occurred in seg2. For seg5 to seg8, we used the same path parameter setting as for the first half. We defined A and W for each path segment as shown in Figure 5.

3.3 Design and Procedure

For *Narrowing*, if W (W_1 or W_2) was too small, the steering times for the seg3, seg4, seg7 and seg8 would be too long. Thus, even if the path shape affected the time in the width-changing areas, the effect would hardly appear in the total MT for the entire loop. On the other hand, if the W was too large, users would not have to pay attention to the path boundaries and the steering time would not be affected by W [1, 17, 35]. This did not match our goal for the current experiment and thus we chose the following three levels for W: 7, 12, and 20 mm. The values for W_1 and W_2 were chosen independent of these values. Thus, if $W_1 = W_2$, the *Shape* condition was defined as *Constant*. If $W_1 > W_2$, it was *Narrowing*, and if $W_1 < W_2$, *Widening*. In other words, the *Shape* condition was defined a posteriori.

We fixed A_1 to 150 mm, the A_2's to 30, 90, and 150 mm, the A_3's to $2W_2$ and $8W_2$, and A_4 to 30 mm. If A_3 is too short, users effectively cannot accelerate for *Widening*, because users might need to pre-plan for the corner between seg3 and seg4 while steering through seg2. To test this assumption, we included two ratios relative to W_2 for A_3.

The combinations yielded $3_{A_2} \times 2_{A_3} \times 3_{W_1} \times 3_{W_2} = 54$ different path configurations. One *block* consisted of the 54 configurations, which appeared in a random order. After 10 randomly selected configurations for practice trials, each participant performed five data-collection blocks. In total,

we recorded $54_{\text{configurations}} \times 5_{\text{blocks}} \times 12_{\text{participants}} = 3240$ data points. Experiment 1 took about 40 min per participant.

3.4 Results

3.4.1 Error Rate and MT. After removing 12 invalid trials due to pen lifting, we were left with data for 3498 trials, including 259 error trials (7.40%). One trial was not recorded due to a system issue. We observed no selection errors where participants did not include orange objects or included green objects. Steering error rates for *Constant*, *Narrowing*, and *Widening* were 6.67, 7.97, and 9.35%, respectively. The mean *MT*s were 4467, 4390, and 5458 msec, respectively.

It is likely that *Widening* was the most difficult condition. However, for example, when $W_1 = 7$ mm and $W_2 = 20$ mm, participants had to keep a low speed in seg1, and the high speed in seg3 could only be maintained for a short time. As shown by this example, W_1 and W_2 thus affected the total difficulty of the path in addition to the width-varying areas. Thus, analyzing statistically significant differences for error rate and *MT* by using an ANOVA with four independent variables (A_2, A_3, W_1, and W_2) or using *Shape* is not meaningful for our purpose. Consequently, we only noted the mean values of them and this decision does not affect our overall goal of comparing model fitness.

3.4.2 Candidate Models. First, the global steering model considers a lassoing task to be a single steering motion. For constant-width path segments, we used $ID_s = A/W$, and for narrowing or widening segments, we used Equation 3. The steering constants (a_s and b_s) are consistent regardless of the *Shape*. Thus, we obtain:

$$MT = [a_s + b_s(ID_s \text{ of seg1})] + [a_s + b_s(ID_s \text{ of seg2})] + \cdots + [a_s + b_s(ID_s \text{ of seg8})] = a'_s + b_s(\text{sum of eight } ID_s \text{ values}) \quad (4)$$

where $a'_s = 8a_s$, but these are constants and thus no distinction is needed. Hence, as the baseline Model #1, the global steering law model uses only a single explanatory variable, ID_s, which is the sum of ID_s for path segments seg1 to 8.

$$MT = a_s + b_s(ID_s), \text{ Model \#1} \quad (5)$$

Next, we test a segmented version of the steering law model that uses different intercepts and slopes to each path segment. Path segmentation has two possible approaches: using different slopes for each path *Shape* condition or using different intercepts. The idea of using different slopes or intercepts follows from Yamanaka and Miyashita's work: the *MT*s for steering through narrowing and widening segments are different [42, 43].

For Model #2, the steering difficulty ID_s is thus split for each path shape; we use subscript *sc* for "Steering through Constant-width path segment", so the ID_{sc} is the sum of ID_s of constant-width path segments and b_{sc} is its slope. In the same manner, the ID_{sn} and ID_{sw} are the sum of ID_s values of narrowing and widening path segments, respectively, and b_{sn} and b_{sw} are their slopes.

$$MT = a_s + b_{sc}(ID_{sc}) + b_{sn}(ID_{sn}) + b_{sw}(ID_{sw}), \text{ Model \#2} \quad (6)$$

For example, in the *Shape* = *Constant* condition, $ID_{sn} = ID_{sw} = 0$. With *Shape* = *Narrowing*, the ID_s for seg2 and seg6 are replaced with ID_{sn}, as computed by Equation 3. This model used the same intercepts for different *Shape* conditions (a_s).

Model #3 uses different intercepts for each *Shape*. In this method, the numbers of path segments for the three *Shapes* matter. We note the number of constant, narrowing, and widening path segments as $\#sc$, $\#sn$, and $\#sw$, respectively, needing only a single steering slope, b_s:

$$MT = a_{sc}(\#sc) + a_{sn}(\#sn) + a_{sw}(\#sw) + b_s(ID_s), \text{ Model \#3} \quad (7)$$

Accounting for both different intercepts and slopes, we obtain:

$$MT = a_{sc}(\#sc) + b_{sc}(ID_{sc}) + a_{sn}(\#sn) + b_{sn}(ID_{sn}) + a_{sw}(\#sw) + b_{sw}(ID_{sw}), \text{ Model \#4} \quad (8)$$

For the *Constant* condition, #*sc* is 4, because seg1–3 merge into a single constant-width path, and so do seg5–7. For *Narrowing*, #*sc* is 6 and #*sn* is 2 and conversely for *Widening*, #*sc* is 6 and #*sw* is 2.

Finally, we generate four additional models from Models #1–4 by taking cornering motions into account. Turning a corner in a path is a kind of pointing task and thus modeled by Fitts' law [26]. For example, when turning the corner after seg3 for *Narrowing* (see Figure 5b), the pointing *MT* is computed as $MT = a_p + b_p \log_2 (A_3/W_2 + 1)$. No pointing motion is required for the final path segment.

However, two modifications are needed. Because the number of cornering motions is always three, i.e., constant, we do not need to consider the number of pointing motions "#*p*" or an intercept of pointing a_p, which are merged by other intercepts. Hence, the final form of Model #5, the "Steering (global model) + Fitts" version of Model #1 is:

$$MT = a + b_s(ID_s) + b_p(ID_p), \quad \text{Model \#5} \tag{9}$$

where a means the sum of $a_s + a_p$, and ID_p is the sum of three pointing difficulty values. Similarly, adding Fitts term to Models #2–4 results in Models #6–8:

$$MT = a + b_{sc}(ID_{sc}) + b_{sn}(ID_{sn}) + b_{sw}(ID_{sw}) + b_p(ID_p), \quad \text{Model \#6} \tag{10}$$

$$MT = a + a_{sn}(\#sn) + a_{sw}(\#sw) + b_s(ID_s) + b_p(ID_p), \quad \text{Model \#7} \tag{11}$$

$$MT = a + b_{sc}(ID_{sc}) + a_{sn}(\#sn) + b_{sn}(ID_{sn}) + a_{sw}(\#sw) + b_{sw}(ID_{sw}) + b_p(ID_p), \quad \text{Model \#8} \tag{12}$$

3.4.3 Statistical Comparison of the Models. To compare the fitness of candidate models, we use adjusted R^2. The adjusted R^2 metric, however, does not give us a clear criterion to judge which model is statistically better than others. To address this, we also compare models through the Akaike Information Criterion *AIC* [5], the *AIC* with small sample size correction (*AICc*) [33], and the Bayesian Information Criterion *BIC* [18]:

$$AIC = -2M + 2K \tag{13}$$

$$AICc = AIC + 2K(K+1)/(N-K-1) \tag{14}$$

$$BIC = -2M + K \ln(N) \tag{15}$$

where M is the maximum log likelihood value of the model, K is the number of free parameters, and N is the number of data points to be regressed (i.e., the number of path configurations; 54 in Experiment 1).

These statistical methods balance the number of coefficients and the fitness to identify a comparatively best model. A model with a lower *AIC* value is a better one and one with $AIC \geq (AIC_{\text{minimum}} + 10)$ can be safely rejected [5]. The same decision criteria are also applicable to *AICc*. *BIC* differences of 0–2 are not significant, 2–6 positive, 6–10 strong, and >10 are very strong [18]. Models with larger adjusted R^2 and smaller *AIC*, *AICc*, and *BIC* values are better. The *AIC* and *AICc* penalize using additional free parameters less, while the *BIC* penalizes this the most.

Table 1 lists the results of model fitting. As demonstrated by the results, using different intercepts or slopes for each *Shape* improves the fitness (Models #2 and #3). Model #3 showed the best fit with all fitness indicators (adjusted R^2, *AIC*, *AICc*, and *BIC*). Yet, combining both ideas (Model #4) did not significantly improve the fitness in terms of *AIC*, *AICc*, and *BIC*, nor did adding the cornering difficulty ID_p. Moreover, models with less variables are easier to use and require less work to identify coefficients. Thus, we believe there is no benefit to adding the Fitts term.

3.5 Discussion of Experiment 1

The results show that considering the path shape significantly improved model fitness. The global steering law model (Model #1) showed adjusted $R^2 = 0.944$, and individual *Shape* conditions showed

Table 1. Model fitting results with 95% CIs [lower, upper] and t values for the coefficients in Experiment 1. Significance values for the coefficients are annotated as *** $p < 0.001$, ** $p < 0.01$, and * $p < 0.05$.

Model	Eq.	Coefficients							adj. R^2	*AIC*	*AICc*	*BIC*
(#1) Steering (global model)	5	a_s: 698 [411, 986] $t = 4.88^{***}$	b_s: 67.6 [63.1, 72.2] $t = 30.0^{***}$						0.944	782	782	786
(#2) Steering (diff. slopes)	6	a_s: 100 [70.7, 130] $t = 6.81^{***}$	b_{sc}: 67.9 [65.0, 70.8] $t = 47.5^{***}$	b_{sn}: 72.3 [61.7, 83.0] $t = 13.6^{***}$	b_{sw}: 66.4 [56.4, 76.3] $t = 13.4^{***}$				0.977	760	761	770
(#3) Steering (diff. intercepts)	7	a_{sc}: 79.2 [16.3, 142] $t = 1.23^{*}$	a_{sn}: 189 [60.6, 318] $t = 2.95^{**}$	a_{sw}: 80.2 [-32.9, 193] $t = 1.42$	b_s: 69.2 [65.5, 72.9] $t = 37.6^{***}$				0.978	753	754	761
(#4) Steering (segmented)	8	a_{sc}: 78.5 [7.53, 149] $t = 2.22^{*}$	b_{sc}: 69.3 [65.0, 73.6] $t = 32.4^{***}$	a_{sn}: 244 [53.0, 435] $t = 2.57^{*}$	b_{sn}: 62.2 [49.0, 75.4] $t = 9.46^{***}$	a_{sw}: 35.1 [-134, 205] $t = 0.416$	b_{sw}: 75.4 [62.1, 88.6] $t = 11.4^{***}$		0.977	755	757	767
(#5 Steering (global)+Fitts	9	a: 867 [609, 1125] $t = 6.75^{***}$	b_s: 71.8 [67.5, 76.1] $t = 33.4^{***}$	b_p: -131 [-190, -72.0] $t = -4.45^{***}$					0.959	766	767	772
(#6) Steering (diff. slopes) + Fitts	10	a: 820 [518, 1122] $t = 5.46^{***}$	b_{sc}: 69.5 [63.1, 76.0] $t = 21.7^{***}$	b_{sn}: 76.2 [63.6, 88.7] $t = 12.2^{***}$	b_{sw}: 75.8 [65.4, 86.1] $t = 14.7^{***}$	b_p: -93.5 [-194, 6.88] $t = -1.87$			0.958	769	770	779
(#7) Steering (diff. intercepts) + Fitts	11	a: 60.3 [-386, 507] $t = 0.271$	a_{sn}: 379 [198, 560] $t = 4.22^{***}$	a_{sw}: 227 [97.8, 356] $t = 3.53^{***}$	b_s: 67.4 [62.9, 71.9] $t = 30.0^{***}$	b_p: 77.5 [-34.4, 189] $t = 1.39$			0.969	753	755	763
(#8) Steering (segmented) + Fitts	12	a: 49.3 [-397, 495] $t = 0.223$	b_{sc}: 66.3 [60.5, 72.1] $t = 23.1^{***}$	a_{sn}: 426 [230, 621] $t = 4.38^{***}$	b_{sn}: 62.8 [49.7, 75.9] $t = 9.67^{***}$	a_{sw}: 168 [19.8, 317] $t = 2.28^{*}$	b_{sw}: 76.4 [63.2, 89.5] $t = 11.7^{***}$	b_p: 93.8 [-29.3, 217] $t = 1.53$	0.969	755	757	768

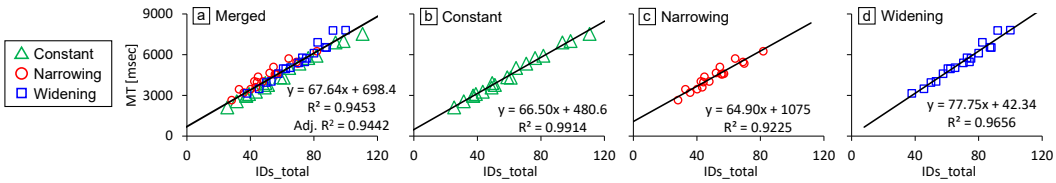

Fig. 6. Model fitness for the entire *MT* using the global steering law model in Experiment 1.

the R^2 values 0.991, 0.923, and 0.966 for *Constant*, *Narrowing*, and *Widening*, respectively (Figure 6). Because the global steering law model takes width changes of the path into account [1], this is not unexpected.

The same tendency also holds for the width-changing area (seg2 and seg6). As an example, if we only analyze seg2, the model fitness using Equation 2 is good for *Constant* ($R^2 = 0.998$), *Narrowing* ($R^2 = 0.945$), and *Widening* ($R^2 = 0.999$), see Figure 7. This poses the question if participants' steering motions were consistent in all *Shape* conditions? To better understand their behaviors, we analyzed the speed profiles from the start to the first corner (seg1–3), as shown in Figure 8. As the raw data were very noisy, we re-sampled the pen-tip trajectory every 5 mm. Also, to better compare the speed differences in the width-changing area, we align the start and end positions of seg2 on the x-axis in Figure 8.

Figure 8a shows that the participants used appropriate speeds for the given path width, i.e., the speed increased as the path width increased. Then, anticipating the corner after seg3, they already began to decelerate in seg2.

Figure 8b shows that, at the end of seg2, the two speed profiles for $W_2 = 7$ mm (orange and blue) match. It is interesting that, although the W_1's for the green and orange conditions are equal (both 20 mm), the speeds at the beginning of seg2 are different, as indicated by the red rectangle. It seems that participants began adjusting to a speed appropriate for the end width W_2 at (or even before)

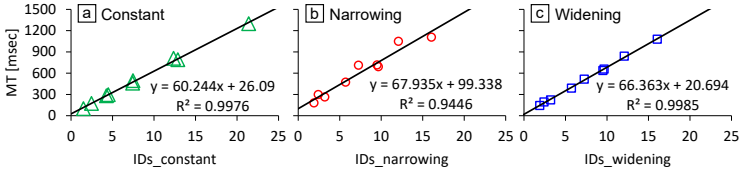

Fig. 7. Model fitting for the upper width-changing area (seg2) in Experiment 1.

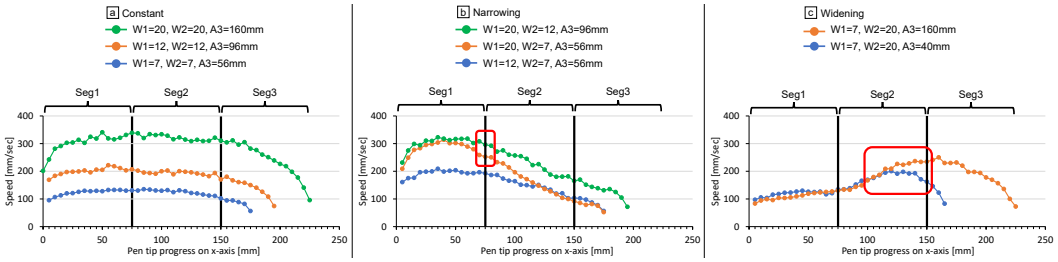

Fig. 8. Speed profiles in seg1–3 in Experiment 1. A_2 is fixed to 150 mm. Black vertical bars show the start and end positions of seg2. Due to the width differences in the preceding seg8, the speed in the first re-sampled points is not aligned.

the start of seg2. This behavior, i.e., deceleration in anticipation of the future path, has been also observed in previous work [42, 43, 46].

Figure 8c supports our decision to use two ratios for A_3, i.e., $2W_2$ or $8W_2$. That is, when A_3 is long, the participants could effectively accelerate in the widening path (orange), as observed in previous work [42, 43, 46]. In contrast, if A_3 is short, they had to start decelerating earlier in seg2 (blue), see the red rectangle.

In summary, participant behaviors were quite different depending on the path width (Figure 8a), the degree of the change of width (b), the length of the future path (c), and path *Shape* (a–c). Hence, although a single dependent variable ID_s achieved adjusted $R^2 = 0.944$, this results does not mean that the participants behaved the same with the three path *Shapes*. In spite of these behavioral differences, the global steering law model still adequately captured the entire MTs with somewhat limited accuracy. Still, in accordance with the *AIC*, *AICc*, and *BIC* criteria for our results, we can confirm that path segmentation significantly improved the prediction accuracy of MT, which supports our hypothesis.

4 EXPERIMENT 2: PATHS INCLUDING STEP-WISE NARROWING AND WIDENING SEGMENTS

In this experiment, the lasso path included two (practically) unconstrained areas as shown in Figure 9. As steering through successive constrained and unconstrained areas had been investigated in previous work [47], we investigate the effect of another path element on the whole lasso time: the transition between constrained and unconstrained areas.

Previous studies focused on whether it is appropriate to use the steering or crossing law models for a given path segment [45, 47]. Typically, the crossing law model predicted entering a constrained area from an unconstrained one better, while the steering law model was more appropriate for passing through a long constrained area. Yet, it is still unclear how the widths and lengths of transition areas affect model fitness. Hence, our goal in Experiment 2 was to investigate the speed

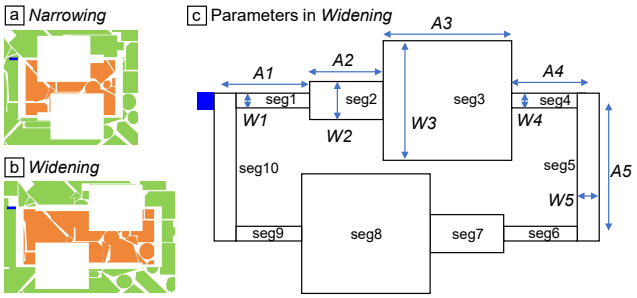

Fig. 9. Path parameter definitions for Experiment 2.

change around transition areas, and thus we focused our experimental design on exploring path parameters for such transitions.

4.1 Participants and Apparatus

Twelve participants (including seven new students) were recruited from a local university (2 female, 10 male; M = 22.2 and SD = 1.72 years). All were right-handed. Each participant received the equivalent of 46 USD for their time. We used the same apparatus as in Experiment 1.

4.2 Task, Design, and Procedure

The task was very similar to that in Experiment 1, but without the *Constant* conditions. For *Narrowing*, seg2 and seg7 were unconstrained areas (seg3 and seg8 for *Widening*), and seg3 and seg8 transition areas (respectively, seg2 and seg7).

We fixed A_1 to 40 mm and W_1 to 7 mm. For *Narrowing*, in seg2, we set A_2 to 140 mm and W_2 to 120 mm. In seg3, we set A_3 to 17, 35, 70, and 140 mm, and W_3 to 12, 17, 22, and 27 mm. For *Widening*, we swapped the values of A_2 and A_3 as well as W_2 and W_3. A_4 and W_4 were the same as A_1 and W_1, respectively. A_5 was 150 mm and W_5 was 20 mm.

We also identified during the experimental design process that the length A of transition areas must vary sufficiently to be able to investigate the effect of such areas. As a rule of thumb, when a steering path's distance is shorter than $5W$, closed-loop motions are not required [31, 35]. Hence, in a *Narrowing* scenario, if $A_3 < 5W_3$, we assume that the operation in seg3 is not steering, but a crossing motion to enter seg4. Otherwise, i.e., $A_3 \geq 5W_3$, a steering movement is needed in seg3. Therefore, A_3 needs to range from less than ($5 \times W_{3_{\text{min}}}$ =) 60 mm to longer than ($5 \times W_{3_{\text{max}}}$ =) 135 mm.

In total, each of the two *Shape* conditions consisted of four As and four Ws in the respective transition areas. Exploring all combinations, one *block* included 32 different configurations ($2_{Shapes} \times 4_A \times 4_W$) appearing in random order. Each participant trained until they successfully executed ten practice trials, followed by six data collection blocks. We recorded $32_{\text{configurations}} \times 6_{\text{blocks}} \times 12_{\text{participants}} = 2304$ data points. Experiment 2 took about 30 min per participant.

4.3 Results

After removing 12 invalid trials that involved lifting the stylus, we identified 226 steering errors (8.93%). The steering error rates for *Narrowing* and *Widening* were 8.13 and 9.72%, respectively. We observed no errors where participants did not include orange objects or included green objects. The mean MTs for *Narrowing* and *Widening* were 5466 and 5367 msec, respectively. As mentioned for

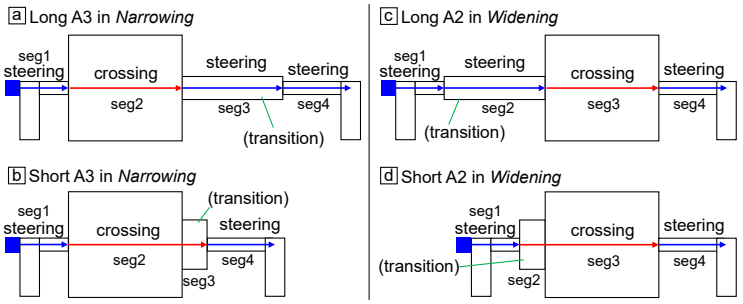

Fig. 10. Performance models depend on the width and length of the transition area for Model #3 in Experiment 2.

Experiment 1, analyzing statistically significant differences for error rate and MT is not meaningful for our purpose, and thus we list only mean values.

For model derivation, the number of corners was again fixed to 3. In addition, and as the corresponding length and width were fixed, the sum of cornering difficulties was always the same among the 32 task configurations. Therefore, we did not use variables $\#p$ and ID_p in this experiment. We arrived at the following four models:

$$MT = a_s + b_s(ID_s), \quad \text{Model \#1} \tag{16}$$

$$MT = a + b_s(ID_s) + b_c(ID_c), \quad \text{Model \#2} \tag{17}$$

$$MT = a_s(\#s) + b_s(ID_s) + a_c(\#c) + b_c(ID_c), \quad \text{Model \#3} \tag{18}$$

$$MT = a + b_{sc}(ID_{sc}) + b_c(ID_c) + a_{sn}(\#sn) + b_{sn}(ID_{sn}) + a_{sw}(\#sw) + b_{sw}(ID_{sw}), \quad \text{Model \#4} \tag{19}$$

Table 2 lists the results for Models #1 to #4. First, for the global steering law model, Model #1, we applied the actual width $A/W = 140/120$ for ID_s in unconstrained areas. As such a wide width does not limit steering speed, the steering law model does not hold [1, 13, 17] and we can replace the width with infinity, which results in $ID_s = 0$. Yet, due to the fixed A and W for these areas, the intercept and slope balance each other and result in the same model fitness.

Second, for Model #2, after segmenting the path into seg1–10, we apply the crossing law model for entering from an unconstrained area into a constrained one. For *Narrowing*, the movement amplitude is A_2, and the width to be crossed is W_3, thus $ID_c = \log_2(A_2/W_3 + 1)$. Similarly, for *Widening*, $ID_c = \log_2(A_3/W_4 + 1)$. Because the $\#s$ and $\#c$ are fixed, a_s and a_c are absorbed by the general intercept a.

Third, we consider the A and W of transition areas. If those areas are narrow and long, they require a steering motion, as shown in Figure 10a and c. Then, the task difficulty for the entire task is defined by Model #3. Yet, if they are short, for *Narrowing* (Figure 10b), the participants perform a crossing motion from the unconstrained area to seg4. Then, the task difficulty for seg2–3 is $ID_c = \log_2((A_2 + A_3)/W_4 + 1)$. Similarly, if the transition for *Widening* is short, (Figure 10d), the participants performed a crossing motion from seg2. We again adopt a threshold based on the $5W$ criterion [31, 35]; with segments with $A < 5W$ being short and not requiring a steering motion.

Finally, in Model #4, if the transition area is short, we approximate the motion in that area as a narrowing/widening path. The crossing law model was originally applied to a motion where users cross a goal line, without a constraint after the goal [1, 4, 7]. Yet, in our present task, the participants also had to pay attention to the path boundaries after the crossing motion, as depicted in Figure 10. Therefore, if the transition area is short ($A < 5W$), we use the steering law model for

Table 2. Model fitting results with 95% CIs [lower, upper] and t values for the coefficients in Experiment 2. Significance values for the coefficients are annotated as *** $p < 0.001$, ** $p < 0.01$, and * $p < 0.05$.

Model	Eq.	Coefficients							adj. R^2	AIC	$AICc$	BIC
(#1) Steering (global)	16	a_s: 1604 [1072, 2135] $t = 6.16^{***}$	b_s: 80.2 [69.1, 91.3] $t = 14.8^{***}$						0.875	426	427	429
(#2) Crossing for unconstrained areas	17	a: 2108 [1555, 2661] $t = 7.79^{***}$	b_s: 81.4 [70.9, 91.8] $t = 15.9^{***}$	b_c: -49.5 [-93.9, -5.097] $t = -2.28$					0.890	423	424	427
(#3) Continuous crossing for transition areas if it is short	18	a_s: 449 [226, 672] $t = 4.23^{***}$	b_s: 31.8 [-0.573, 64.1] $t = 2.01$	a_c: -13.3 [-136, 109] $t = -0.223$	b_c: 119 [68.2, 169] $t = 4.82^{***}$				0.786	444	446	450
(#4) Approximate narrowing or widening shapes for transitions	19	a: 3649 [2625, 4673] $t = 7.34^{***}$	b_{sc}: 50.4 [31.8, 69.1] $t = 5.57^{***}$	b_c: -34.3 [-91.7, 23.2] $t = -1.23$	a_{sn}: -295 [-454, -137] $t = -3.85^{***}$	b_{sn}: 63.1 [39.2, 87.0] $t = 5.43^{***}$	a_{sw}: -262 [-438, -85.7] $t = -3.06^{**}$	b_{sw}: 55.4 [30.9, 79.8] $t = 4.67^{***}$	0.937	409	413	419

narrowing/widening path shapes (Equation 3). Because the number of crossing motions is fixed to 2, and $\#sc$ is fixed to $8 - (\#sn) - (\#sw)$, we do not include them and only use a general intercept a.

In contrast to the results for Experiment 1, the global steering law model did not show a good fit (Model #1). Although we attempted to use the crossing law model for unconstrained areas (Model #2), the fitness did not improve significantly over Model #1, which contradicts results from a previous study on gird-icon lassoing [45]. We initially believed that Model #3 could more closely model user behaviors in the transition areas, but we found that it degraded the fitness even more. The significantly best model according to the *AIC*, *AICc*, and *BIC* measures was Model #4. Thus, we can say that closely approximating the motion within transition areas resulted in a more desirable MT prediction accuracy.

To illustrate how well Model #4 outperforms the other candidates, we show the regression graphs in Figure 11. For obtaining 2D graphs from regressions with two or more explanatory variables, we aggregated the coefficients and variables. For example, for Model #2, we converted the obtained coefficients as follows.

$$MT = 2108 + 81.4 \cdot ID_s - 49.5 \cdot ID_c = 2108 + 81.4(ID_s - 0.608 \cdot ID_c), \quad \text{Model \#2} \tag{20}$$

Similarly, Models #3 and #4 became as follows, respectively.

$$MT = 449(\#s + 0.0707 \cdot ID_s - 0.0297 \cdot \#c + 0.264 \cdot ID_c), \quad \text{Model \#3} \tag{21}$$

$$MT = 3649 + 50.4(ID_{sc} - 0.680 \cdot ID_c - 5.86 \cdot \#sn + 1.25 \cdot ID_{sn} - 5.19 \cdot \#sw + 1.10 \cdot ID_{sw}), \quad \text{Model \#4} \tag{22}$$

We call the value inside the brackets $ID_{\text{corrected}}$, which is the x-axis value in the graphs. We can see that most data points in Figure 11d (Model #4) are located close to the regression line. This tendency also holds for Models #1 and #2, but some points are still away from their regression lines.

4.4 Discussion of Experiment 2

To analyze the user behaviors in the transition areas, we again re-sampled the pen tip trajectory every 5 mm as shown in Figure 12. As expected, when the transition areas were long for *Narrowing* (Figure 12a), the speeds in that area (seg3) were stable at first, and then began decelerating to enter the narrow seg4. The initial speeds in seg3 were even lower with narrower W_3. The effect of W_3 can also be seen in seg2 (unconstrained area); as W_3 decreases, the speeds decrease in advance of the joint between seg2 and seg3. Also, in Figure 12b (*Widening*), the speeds in the long transition area

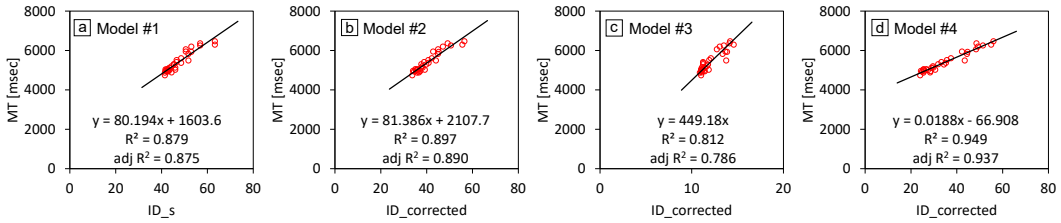

Fig. 11. Linear regressions of the candidate models in Experiment 2. Note that (c) uses a different x-axis than the others.

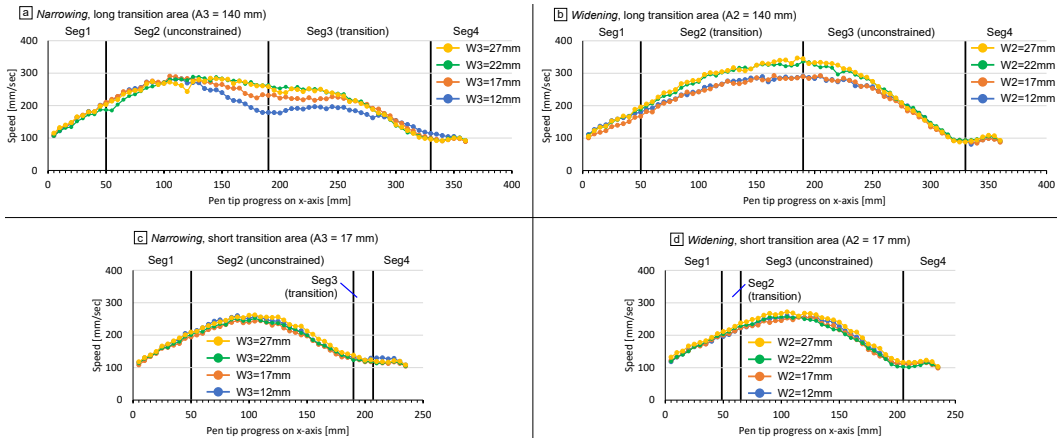

Fig. 12. Speed profiles for different widths (12–27 mm) with long vs. short transition areas in Experiment 2.

gradually increased, and then began decelerating before seg4. In sum, when the transition area was long, the behavior in that area was similar to conventional steering with future-path anticipation.

In contrast, if the transition area was short, no effect of the width of the transition area was observed on the speed in seg2 and seg3 (Figure 12c and d). This confirms that the users exhibited different strategies for long (Figure 12a and b) and short transition areas (c and d). Hence, different models are needed depending on the length of such areas, and Models #1 and #2 did not account for this difference, resulting in lower fitness.

Model #3 replaces the steering difficulty in the short transition area with a crossing difficulty, which assumes that no steering motion occurred in such areas. Yet, Model #3 showed the worst fit among all candidates. We found that using a width-changing steering law model in such transition areas is better (Model #4). Because the width-changing ID_s is used only if the transition area is short, it is difficult to see clearly if the speed profiles in those areas are similar to the actual narrowing/widening path segments, as shown in Figure 8. Looking in the future, the high prediction accuracy of Model #4 motivates us to consider further studies with, e.g., much longer *and* wider transition areas.

5 GENERAL DISCUSSION

5.1 User Performance and Model Fitting

In Experiment 1, the path was constrained so that the participants had to always pay attention to the path boundaries. In that situation, the global steering law model showed adjusted $R^2 = 0.944$

to the experimental data (Model #1 in Table 1). In addition, several augmented versions of the model showed significantly better fits according to the *AIC*, *AICc*, and *BIC* measures. Thus, if the users' strategy and behavior is constrained through a specific path, the lassoing time was more accurately predicted by the path segmentation. For Experiment 2, where unconstrained areas were included, we reached the same conclusion that the path segmentation was effective; the prediction accuracy of the global steering law (Model #1) showed adjusted $R^2 = 0.875$ while the best-fit Model #4 showed adjusted $R^2 = 0.937$ with significantly better *AIC*, *AICc*, and *BIC* results (Table 2).

For the results of Experiment 2, there seems to remain more space to improve the model fitness even further compared to Experiment 1. As the speed profiles of Experiment 2 showed (Figure 12), behaviors in unconstrained and transition areas cannot be clearly explained as steering a constant-width or a narrowing/widening path, nor as crossing a goal. Thus, determining an even more accurate model for each path segment is a challenge for the future.

Although our discussion compares fits on the basis of three information-based criteria, Model #1 (the global steering law model) might exhibit sufficiently *good* fits for some purposes. Thus, the choice of models depends on the tradeoff between the simplicity of the formulation and how much accuracy researchers need. As a model with less variables is easier to use, Model #1 may suffice for researchers who would like to predict *MT*s with (say) adjusted $R^2 > 0.9$. Still, the result of Experiment 2 suggests that we should use Model #4 for the best prediction accuracy, even when using the *AICc* criterion. Yet, we acknowledge that seven free parameters constitutes a complex *MT* prediction model.

We see negative slopes for crossing (b_c) in Models #2 and #4 in Experiment 2 (Table 2). This seemed initially strange but we identified that the reason behind this is that we replaced the crossing difficulty with a steering difficulty in our model. As increasing the ID_c means that the steering motion phase has to decrease – and thus also the overall *MT* – this does not invalidate the model.

5.2 Implications

5.2.1 Prediction of MTs for Untested Task Conditions to Estimate the Efficiency of Lasso and Target/Command Selection Techniques. Based on our results, and in the same manner as other performance models, we can predict how the *MT* changes with specific task conditions or novel interaction techniques. Based on reflections what our outcomes mean, illustration software could, once a user selects the lasso selection tool, automatically shrink all object sizes to widen the path to make lassoing easier [46]. Another possibility to support lassoing operations is to automatically trigger magnification for dense areas, similar to an approach proposed for target pointing [24].

Our models can predict the magnitude of such improvements, e.g., when the path is widened. For example, in a *Narrowing* condition in Experiment 1, if we use the path parameters of $A_1 = 150$, $A_2 = 150$, $A_3 = 2W_2$, $A_4 = 30$, $W_1 = 20$, and $W_2 = 7$ mm, we can then predict the *MT* based on the best Model #3 in Table 1 as 4519 ms. When we widen W_2 to 15 mm, we obtain $MT = 3734$ ms, which corresponds to a reduction of 17%.

This application of our work also generalizes to target and command selection techniques that involve stroking through the intended objects, such as *Bubble Clusters* [39], *Pins 'n' Touches* [32], *CrossY* [6], *Attribute gates* [34], *Don't click, paint!* [9], and *Crossets* [27]. For example, in *Bubble Clusters* and *Pins 'n' Touches*, a user can group many icons by passing through desired ones with a single continuous stroke. Touching non-target icons needs to be avoided because this then requires subsequent operations (to undo or ungroup).

Although previous work has measured the *MT* for such operations experimentally with a fixed icon size [39], and as we empirically showed above, their results should be affected by the geometry of the stroke such as the width of the path to be steered. Based on our results, researchers can compute, e.g., the potential increase in the *MT* if a path to be steered is narrowed from 30 to 20

mm, without needing to run another experiment. Our work informs researchers who would like to propose novel lasso techniques by enabling the prediction of the performance without conducting (potentially costly) user studies.

5.2.2 Development of Novel Interaction Techniques and Modeling MTs. As we imposed no fundamental restrictions on the object shapes, the results of our work are also very likely to hold for width-varying paths around groups of icons or other rectangular objects, which generalizes previous work on lassoing for such objects. As one can approximate curved path boundaries with polygons, we also believe that our approach might generalize to arbitrary object shapes. Yet, such a theoretically possible generalization will need to be verified in the future, especially for approximations that involve many small path segments.

Beyond lasso tasks, another potential application of our work is to model the *MT*s for making strokes. For example, gesture-based menu navigation techniques [20], where, based on the steering law, the authors identified that their new technique reduces the *MT*.

Developing and evaluating other new UIs, e.g., for sketching in Virtual Reality environments [8], also relies on existing performance models, e.g., a pen gesturing model [11], which is again based on the steering law. Based on our outcomes, UI developers and researchers can predict *MT*s for novel gesturing/stroking interaction techniques in tasks with width-changing paths and unconstrained areas, tasks that were not covered by previous work.

5.2.3 Design Considerations for Novel Interaction Techniques. Previous studies on selecting multiple objects with a single stroke sometimes conducted user experiments without controlling the target size as mentioned above [6, 9, 27, 34]. Our results suggest that simply making each item larger for a crossing-based technique reduces the task completion time. Although *MT*s in wider paths for lasso-techniques are known to be shorter according to the steering law and its variations, the investigated path configurations were limited to a fixed width with linear or circular shape [1, 2, 30, 42, 45] or a width-changing but linear shape [42, 46]. Accordingly, researchers could simply enlarge each item for object-selection techniques to effectively reduce *MT*s on the basis of the steering law, yet our work is the first to empirically verify this assumption for whole lasso motions.

Another promising technique to reduce *MT*s in lasso tasks is to shrink objects that are located in the forward direction of the cursor's movement (thus widening the path to be steered) so that users have to pay less attention to hitting unwanted objects [46]. Yet, using this idea causes problems when there is a corner immediately ahead after the shrunk objects. Then, and although the path width of the current cursor position is wide, the speed cannot be increased, which was confirmed by our speed-profile analysis results. From this point of view, it is (too) optimistic to assume that the movement speed could be increased by expanding the path in the forward direction [46].

For techniques that enlarge targets to be crossed by the cursor [6, 9, 27, 34] or widen the path so that the cursor more easily steers between unwanted targets [46], where the dynamic change in size occurs depending on the cursor position or direction, users have to respond on-line, which in turn carries the risk of lowering performance (see Gutwin's study on fish-eye target resizing [16]). For illustration software, there is also the concern that if content shrinks too much, users may not be able to tell which image they wanted to select.

The issue of how humans respond on-line during deliberate stroke movements raises the question at which distance from the current cursor position forward path segments (or objects) should change so that the user can react in time. Our Experiment 1 used relatively tighter paths than Experiment 2, and Figure 8b suggests that the participants began to change the speed already more than 30 mm before the width-changing point. In contrast, in Experiment 2, Figure 12a suggests that, even when the cursor was in the unconstrained area, the participants began to decelerate already more than

90 mm before entering the transition area. These results point out that users anticipated further ahead for the higher speed. It would thus be interesting to determine how far ahead each object's size should be changed depending on the current speed. It is also possible to combine this idea with Sloppy Selection [21], which determines the lasso-selection width based on the current speed.

Thus, simply changing each target's size may not be a good idea for trajectory-based object selection techniques, as fine-tuning several parameters would be needed to improve user performance. One possible solution is to keep the visual size constant and to only change the motor (collision) size. However, if the visual appearance is kept, users may not be able to effectively utilize the motor space path-width change, and thus *MT*s may not become smaller. This issue needs to be investigated in the future.

5.3 Limitations and Future Work

Our results are potentially limited by the experimental conditions, such as using fixed path lengths in some segments and involving a constant number of corners. In addition, width-changing, unconstrained, and transition areas appeared only during rightward and leftward movements to control the possible effects of hand occlusion. In realistic lasso tasks, such areas would appear at various positions and directions, and thus some modifications of the models might be needed. One reason is that, for constant-width linear-path steering tasks, *MT*s can differ depending on the movement directions; horizontal movements were significantly faster than vertical ones [35, 48]. Assuming that the *MT*s in width-changing path segments also differ depending on the direction (horizontal or vertical), we would need to use different coefficients, such as using an intercept for steering through a horizontal narrowing path segment (a_{sn_h}) and a vertical one (a_{sn_v}).

In our experimental conditions, all corners were right angled (90°), but realistic lasso tasks may involve more gradual and acute ones. There, existing performance models might be used, e.g., different steering law models for varying curvature radii [25, 44] and a velocity prediction model based on the stroke curvature in unconstrained areas [15, 38].

Although our participants were all right-handed, we assume that the models examined in this paper are applicable to left-handed users (potentially with different coefficient values), but speed profiles might change from those illustrated in Figures 8 and 12. For example, because we fixed the start position to the top-left of the path, left-handed users can see the whole first straight region (seg1–3 in Experiment 1 and seg1–4 in Experiment 2), which would enable them to accelerate more than right-handed users.

Several potentially necessary factors for modeling lasso times are listed below, with potential solutions to improve the prediction accuracy in the future.

(1) Pen movement speeds and *MT*s depend on the movement direction θ in path steering tasks [35]. This previous work found that the *MT*s changed symmetrically and thus proposed a refinement model: $MT = a + (b + c \cdot \sin\theta)(A/W + d)$. Incorporating such a term might be particularly needed for paths that have many twists and turns.

(2) In our experiments the horizontal movement parts were longer than the vertical ones. Thus, the left- and rightward strokes involved (somewhat) larger arm movements. In this context, it is known that the scale effect matters for path steering operations [3, 30]. That is, the *MT* tends to be short when the task can be accomplished within the "natural movement area for the hand", while too large or small movements become difficult for humans. Senanayake et al. [30] proposed the following relationship between the slope of the steering law ("b" in $MT = a + b \cdot ID_s$) and the scale: $1/b = k_0 \cdot \text{scale}^2 + k_1 \cdot \text{scale} + k_2$, where k_0–k_2 are coefficients. According to this, it might be better to use different steering coefficients depending on the segment length.

(3) Our participants changed the speed much in advance of the end of the current path segment. For example, as shown in Figure 8b and c, when a corner was located after seg3 the user's speed

already changed even before they entered seg2 (Figure 8b) or in the middle of seg2 (c). While human corrective reaction time is known, e.g., 190 to 260 msec [19], we know presently no method to reliably predict the initial timing of such decelerations or accelerations.

These factors should affect (only) the prediction of *MT*s for each path segment, and previous work proposed appropriate models for each condition as mentioned above. Thus, our overall recommendation of segmenting the whole path and then modeling *MT*s for each segment still holds.

Lastly, we focused on modeling *MT*s in this study in simplified tasks that do not involve the time and cognitive cost to distinguish the targets to be selected, nor the time to point to the starting position (see Section 1.3). Investigating lasso motions in a concrete application might enable observation of more realistic user behaviors and would help to verify the models' applicability, and we are considering this for future work. While we believe that the additional aspects of lasso movements needed for real applications can be well-predicted by existing models (e.g., visual search time [40] and positioning time [14]), further experiments might be needed to confirm this.

6 CONCLUSION

We set out to predict lasso operation times for scenarios where the objects to be selected have non-rectangular shapes and are arranged in non-grid positions, which requires dealing with more general lasso paths. We identified in two experiments that paths with narrowing or widening path segments, be it continuously or step-wise, are best modeled by segmenting the path into segments and modeling each part individually. This result supports our hypothesis that path segmentation is an appropriate approach for movement time prediction of lasso tasks. Based on our results, researchers can more accurately estimate the performance of their novel lasso techniques for specific target arrangements.

REFERENCES

[1] Johnny Accot and Shumin Zhai. 1997. Beyond Fitts' law: models for trajectory-based HCI tasks. In *Proceedings of the SIGCHI Conference on Human Factors in Computing Systems (CHI '97)*. ACM, New York, NY, USA, 295–302. https://doi.org/10.1145/258549.258760

[2] Johnny Accot and Shumin Zhai. 1999. Performance Evaluation of Input Devices in Trajectory-based Tasks: An Application of the Steering Law. In *Proceedings of the SIGCHI Conference on Human Factors in Computing Systems* (Pittsburgh, Pennsylvania, USA) *(CHI '99)*. ACM, New York, NY, USA, 466–472. https://doi.org/10.1145/302979.303133

[3] Johnny Accot and Shumin Zhai. 2001. Scale effects in steering law tasks. In *Proceedings of the SIGCHI Conference on Human Factors in Computing Systems (CHI '01)*. ACM, New York, NY, USA, 1–8. https://doi.org/10.1145/365024.365027

[4] Johnny Accot and Shumin Zhai. 2002. More than dotting the i's — foundations for crossing-based interfaces. In *Proceedings of the SIGCHI Conference on Human Factors in Computing Systems (CHI '02)*. ACM, New York, NY, USA, 73–80. https://doi.org/10.1145/503376.503390

[5] Hirotugu Akaike. 1974. A new look at the statistical model identification. *IEEE Trans. Automat. Control* 19, 6 (Dec 1974), 716–723. https://doi.org/10.1109/TAC.1974.1100705

[6] Georg Apitz and François Guimbretière. 2004. CrossY: A Crossing-based Drawing Application. In *Proceedings of the 17th Annual ACM Symposium on User Interface Software and Technology* (Santa Fe, NM, USA) *(UIST '04)*. ACM, New York, NY, USA, 3–12. https://doi.org/10.1145/1029632.1029635

[7] Georg Apitz, François Guimbretière, and Shumin Zhai. 2008. Foundations for Designing and Evaluating User Interfaces Based on the Crossing Paradigm. *ACM Trans. Comput.-Hum. Interact.* 17, 2, Article 9 (May 2008), 42 pages. https://doi.org/10.1145/1746259.1746263

[8] Rahul Arora, Rubaiat Habib Kazi, Fraser Anderson, Tovi Grossman, Karan Singh, and George Fitzmaurice. 2017. Experimental Evaluation of Sketching on Surfaces in VR. In *Proceedings of the 2017 CHI Conference on Human Factors in Computing Systems* (Denver, Colorado, USA) *(CHI '17)*. Association for Computing Machinery, New York, NY, USA, 5643–5654. https://doi.org/10.1145/3025453.3025474

[9] Patrick Baudisch. 1998. Don't Click, Paint! Using Toggle Maps to Manipulate Sets of Toggle Switches. In *Proceedings of the 11th Annual ACM Symposium on User Interface Software and Technology* (San Francisco, California, USA) *(UIST '98)*. ACM, New York, NY, USA, 65–66. https://doi.org/10.1145/288392.288574

[10] Per Bjerre, Allan Christensen, Andreas Køllund Pedersen, Simon André Pedersen, Wolfgang Stuerzlinger, and Rasmus Stenholt. 2017. Predictive Model for Group Selection Performance on Touch Devices. In *Human-Computer Interaction. Interaction Contexts - 19th International Conference, HCI International 2017, Vancouver, BC, Canada, July 9-14, 2017, Proceedings, Part II*. Springer International Publishing, Cham, 142–161. https://doi.org/10.1007/978-3-319-58077-7_12

[11] Xiang Cao and Shumin Zhai. 2007. Modeling Human Performance of Pen Stroke Gestures. In *Proceedings of the SIGCHI Conference on Human Factors in Computing Systems* (San Jose, California, USA) *(CHI '07)*. Association for Computing Machinery, New York, NY, USA, 1495–1504. https://doi.org/10.1145/1240624.1240850

[12] Hoda Dehmeshki and Wolfgang Stuerzlinger. 2006. Using Perceptual Grouping for Object Group Selection. In *CHI '06 Extended Abstracts on Human Factors in Computing Systems* (Montréal, Québec, Canada) *(CHI EA '06)*. Association for Computing Machinery, New York, NY, USA, 700–705. https://doi.org/10.1145/1125451.1125593

[13] Colin G. Drury. 1971. Movements with lateral constraint. *Ergonomics* 14, 2 (1971), 293–305. https://doi.org/10.1080/00140137108931246

[14] Paul M. Fitts. 1954. The information capacity of the human motor system in controlling the amplitude of movement. *Journal of Experimental Psychology* 47, 6 (1954), 381–391. https://doi.org/10.1037/h0055392

[15] Tamar Flash and Neville Hogan. 1985. The coordination of arm movements: an experimentally confirmed mathematical model. *The journal of Neuroscience* 5, 7 (1985), 1688–1703.

[16] Carl Gutwin. 2002. Improving Focus Targeting in Interactive Fisheye Views. In *Proceedings of the SIGCHI Conference on Human Factors in Computing Systems* (Minneapolis, Minnesota, USA) *(CHI '02)*. Association for Computing Machinery, New York, NY, USA, 267–274. https://doi.org/10.1145/503376.503424

[17] Errol R. Hoffmann. 2009. Review of models for restricted-path movements. *International Journal of Industrial Ergonomics* 39, 4 (2009), 578 – 589. https://doi.org/10.1016/j.ergon.2008.02.007 Special issue: Felicitating Colin G. Drury.

[18] Robert E. Kass and Adrian E. Raftery. 1995. Bayes Factors. *J. Amer. Statist. Assoc.* 90, 430 (1995), 773–795. https://doi.org/10.1080/01621459.1995.10476572

[19] Steven W. Keele and Michael I. Posner. 1968. Processing of visual feedback in rapid movements. *Journal of Experimental Psychology* 77, 1 (1968), 155–158. https://doi.org/10.1037/h0025754

[20] Masatomo Kobayashi and Takeo Igarashi. 2003. Considering the Direction of Cursor Movement for Efficient Traversal of Cascading Menus. In *Proceedings of the 16th Annual ACM Symposium on User Interface Software and Technology* (Vancouver, Canada) *(UIST '03)*. Association for Computing Machinery, New York, NY, USA, 91–94. https://doi.org/10.1145/964696.964706

[21] Edward Lank and Eric Saund. 2005. Sloppy Selection: Providing an Accurate Interpretation of Imprecise Selection Gestures. *Comput. Graph.* 29, 4 (Aug. 2005), 490–500. https://doi.org/10.1016/j.cag.2005.05.003

[22] I. Scott MacKenzie. 1992. Fitts' law as a research and design tool in human-computer interaction. *Human-Computer Interaction* 7, 1 (1992), 91–139. https://doi.org/10.1207/s15327051hci0701_3

[23] Sachi Mizobuchi and Michiaki Yasumura. 2004. Tapping vs. Circling Selections on Pen-based Devices: Evidence for Different Performance-shaping Factors. In *Proceedings of the SIGCHI Conference on Human Factors in Computing Systems* (Vienna, Austria) *(CHI '04)*. ACM, New York, NY, USA, 607–614. https://doi.org/10.1145/985692.985769

[24] Martez E. Mott and Jacob O. Wobbrock. 2014. Beating the Bubble: Using Kinematic Triggering in the Bubble Lens for Acquiring Small, Dense Targets. In *Proceedings of the SIGCHI Conference on Human Factors in Computing Systems* (Toronto, Ontario, Canada) *(CHI '14)*. Association for Computing Machinery, New York, NY, USA, 733–742. https://doi.org/10.1145/2556288.2557410

[25] Mathieu Nancel and Edward Lank. 2017. Modeling User Performance on Curved Constrained Paths. In *Proceedings of the 2017 CHI Conference on Human Factors in Computing Systems* (Denver, Colorado, USA) *(CHI '17)*. ACM, New York, NY, USA, 244–254. https://doi.org/10.1145/3025453.3025951

[26] Robert Pastel. 2006. Measuring the Difficulty of Steering Through Corners. In *Proceedings of the SIGCHI Conference on Human Factors in Computing Systems* (Montréal, Québec, Canada) *(CHI '06)*. ACM, New York, NY, USA, 1087–1096. https://doi.org/10.1145/1124772.1124934

[27] Charles Perin, Pierre Dragicevic, and Jean-Daniel Fekete. 2015. Crossets: Manipulating Multiple Sliders by Crossing. In *Proceedings of the 41st Graphics Interface Conference* (Halifax, Nova Scotia, Canada) *(GI '15)*. Canadian Information Processing Society, CAN, 233–240.

[28] Nicolas Rashevsky. 1959. Mathematical biophysics of automobile driving. *Bulletin of Mathematical Biophysics* 21, 4 (1959), 375–385. https://doi.org/10.1007/BF02477896

[29] Carsten Rother, Vladimir Kolmogorov, and Andrew Blake. 2004. "GrabCut": Interactive Foreground Extraction Using Iterated Graph Cuts. In *ACM SIGGRAPH 2004 Papers* (Los Angeles, California) *(SIGGRAPH '04)*. Association for Computing Machinery, New York, NY, USA, 309–314. https://doi.org/10.1145/1186562.1015720

[30] Ransalu Senanayake and Ravindra S. Goonetilleke. 2016. Pointing Device Performance in Steering Tasks. *Perceptual and Motor Skills* 122, 3 (2016), 886–910. https://doi.org/10.1177/0031512516649717

[31] Ransalu Senanayake, Errol R. Hoffmann, and Ravindra S. Goonetilleke. 2013. A model for combined targeting and tracking tasks in computer applications. *Experimental Brain Research* 231, 3 (01 Nov 2013), 367–379. https://doi.org/10.1007/s00221-013-3700-4

[32] Sven Strothoff, Wolfgang Stuerzlinger, and Klaus Hinrichs. 2015. Pins 'n' Touches: An Interface for Tagging and Editing Complex Groups. In *Proceedings of the 2015 International Conference on Interactive Tabletops & Surfaces (ITS)*. ACM, New York, NY, USA, 191–200. https://doi.org/10.1145/2817721.2817731

[33] Nariaki Sugiura. 1978. Further analysts of the data by akaike' s information criterion and the finite corrections. *Communications in Statistics - Theory and Methods* 7, 1 (1978), 13–26. https://doi.org/10.1080/03610927808827599

[34] Ahmed N. Sulaiman and Patrick Olivier. 2008. Attribute Gates. In *Proceedings of the 21st Annual ACM Symposium on User Interface Software and Technology* (Monterey, CA, USA) *(UIST '08)*. ACM, New York, NY, USA, 57–66. https://doi.org/10.1145/1449715.1449726

[35] Namal Thibbotuwawa, Ravindra S. Goonetilleke, and Errol R. Hoffmann. 2012. Constrained Path Tracking at Varying Angles in a Mouse Tracking Task. *Human Factors* 54, 1 (2012), 138–150. https://doi.org/10.1177/0018720811424743

[36] Namal Thibbotuwawa, Errol R. Hoffmann, and Ravindra S. Goonetilleke. 2012. Open-loop and feedback-controlled mouse cursor movements in linear paths. *Ergonomics* 55, 4 (2012), 476–488. https://doi.org/10.1080/00140139.2011.644587

[37] Hiroki Usuba, Shota Yamanaka, and Homei Miyashita. 2019. Comparing Lassoing Criteria and Modeling Straight-Line and One-Loop Lassoing Motions Considering Criteria. In *Proceedings of the 2019 ACM International Conference on Interactive Surfaces and Spaces* (Daejeon, Republic of Korea) *(ISS '19)*. Association for Computing Machinery, New York, NY, USA, 181–191. https://doi.org/10.1145/3343055.3359707

[38] Paolo Viviani and Tamar Flash. 1995. Minimum-Jerk, Two-Thirds Power Law, and Isochrony: Converging Approaches to Movement Planning. *Journal of experimental psychology. Human perception and performance* 21 (03 1995), 32–53. https://doi.org/10.1037/0096-1523.21.1.32

[39] Nayuko Watanabe, Motoi Washida, and Takeo Igarashi. 2007. Bubble Clusters: An Interface for Manipulating Spatial Aggregation of Graphical Objects. In *Proceedings of the 20th Annual ACM Symposium on User Interface Software and Technology* (Newport, Rhode Island, USA) *(UIST '07)*. Association for Computing Machinery, New York, NY, USA, 173–182. https://doi.org/10.1145/1294211.1294241

[40] Jeremy Wolfe and Todd Horowitz. 2017. Five factors that guide attention in visual search. *Nature Human Behaviour* 1 (03 2017), 0058. https://doi.org/10.1038/s41562-017-0058

[41] Pengfei Xu, Hongbo Fu, Oscar Kin-Chung Au, and Chiew-Lan Tai. 2012. Lazy Selection: A Scribble-based Tool for Smart Shape Elements Selection. *ACM Trans. Graph.* 31, 6, Article 142 (Nov. 2012), 9 pages. https://doi.org/10.1145/2366145.2366161

[42] Shota Yamanaka and Homei Miyashita. 2016. Modeling the Steering Time Difference Between Narrowing and Widening Tunnels. In *Proceedings of the 2016 CHI Conference on Human Factors in Computing Systems* (San Jose, California, USA) *(CHI '16)*. ACM, New York, NY, USA, 1846–1856. https://doi.org/10.1145/2858036.2858037

[43] Shota Yamanaka and Homei Miyashita. 2016. Scale Effects in the Steering Time Difference Between Narrowing and Widening Linear Tunnels. In *Proceedings of the 9th Nordic Conference on Human-Computer Interaction* (Gothenburg, Sweden) *(NordiCHI '16)*. ACM, New York, NY, USA, Article 12, 10 pages. https://doi.org/10.1145/2971485.2971486

[44] Shota Yamanaka and Homei Miyashita. 2019. Modeling Pen Steering Performance in a Single Constant-Width Curved Path. In *Proceedings of the 2019 ACM International Conference on Interactive Surfaces and Spaces* (Daejeon, Republic of Korea) *(ISS '19)*. Association for Computing Machinery, New York, NY, USA, 65–76. https://doi.org/10.1145/3343055.3359697

[45] Shota Yamanaka and Wolfgang Stuerzlinger. 2019. Modeling Fully and Partially Constrained Lasso Movements in a Grid of Icons. In *Proceedings of the 2019 CHI Conference on Human Factors in Computing Systems* (Glasgow, Scotland Uk) *(CHI '19)*. ACM, New York, NY, USA, Article 120, 12 pages. https://doi.org/10.1145/3290605.3300350

[46] Shota Yamanaka, Wolfgang Stuerzlinger, and Homei Miyashita. 2017. Steering Through Sequential Linear Path Segments. In *Proceedings of the 2017 CHI Conference on Human Factors in Computing Systems* (Denver, Colorado, USA) *(CHI '17)*. ACM, New York, NY, USA, 232–243. https://doi.org/10.1145/3025453.3025836

[47] Shota Yamanaka, Wolfgang Stuerzlinger, and Homei Miyashita. 2018. Steering Through Successive Objects. In *Proceedings of the 2018 CHI Conference on Human Factors in Computing Systems* (Montreal QC, Canada) *(CHI '18)*. ACM, New York, NY, USA, Article 603, 13 pages. https://doi.org/10.1145/3173574.3174177

[48] Xiaolei Zhou, Xiangshi Ren, and Hue YUi. 2008. Effect of Start Position on Human Performance in Steering Tasks. In *2008 International Conference on Computer Science and Software Engineering*, Vol. 2. IEEE, USA, 1098–1101. https://doi.org/10.1109/CSSE.2008.1310